

# Monte Carlo comparisons of the self-avoiding walk and SLE as parameterized curves

Tom Kennedy  
Department of Mathematics  
University of Arizona  
Tucson, AZ 85721  
email: [tgk@math.arizona.edu](mailto:tgk@math.arizona.edu)

June 29, 2018

## Abstract

The scaling limit of the two-dimensional self-avoiding walk (SAW) is believed to be given by the Schramm-Loewner evolution (SLE) with the parameter  $\kappa$  equal to  $8/3$ . The scaling limit of the SAW has a natural parameterization and SLE has a standard parameterization using the half-plane capacity. These two parameterizations do not correspond with one another. To make the scaling limit of the SAW and SLE agree as parameterized curves, we must reparameterize one of them. We present Monte Carlo results that show that if we reparameterize the SAW using the half-plane capacity, then it agrees well with SLE with its standard parameterization. We then consider how to reparameterize SLE to make it agree with the SAW with its natural parameterization. We argue using Monte Carlo results that the so-called  $p$ -variation of the SLE curve with  $p = 1/\nu = 4/3$  provides a parameterization that corresponds to the natural parameterization of the SAW.

# 1 Introduction

The scaling limit of the two dimensional self-avoiding walk (SAW) is believed to be the Schramm-Loewner evolution (SLE) with  $\kappa = 8/3$  [13]. Previous Monte Carlo studies have compared the scaling limit of the SAW and  $SLE_{8/3}$  as unparameterized curves [9, 10]. These studies considered random variables that did not depend on how the curve were parameterized and found excellent agreement between the distributions for the SAW and  $SLE_{8/3}$ . The goal of this paper is to use Monte Carlo simulations to understand how the SAW and  $SLE_{8/3}$  curves should be parameterized so that they agree as parameterized curves.

We give a brief definition of the SAW. For a detailed treatment we refer the reader to [17]. The relationship of the SAW to  $SLE_{8/3}$  is the subject of [13]. We restrict our attention to the SAW on a two-dimensional lattice restricted to the upper half plane. Fix a positive integer  $N$ . We consider all nearest neighbor walks which begin at the origin, have exactly  $N$  steps, remain in the upper half plane (except for the starting point) and never visit the same site more than once. There are a finite number of such walks, so we can put the uniform probability measure on this set of walks. We then attempt to construct the scaling limit by the following double limit. We first let  $N \rightarrow \infty$ . For the case of the half-plane this limit was proved to exist in [13], but there is no general proof of its existence. We then take the lattice spacing to zero. This limit has not been proved to exist, but it is believed that it does and gives a measure on curves in the upper half plane which start at the origin and go to  $\infty$ . The SAW curves are simple (do not intersect themselves) by definition. This does not insure that in the scaling limit the measure is supported on simple curves, but it is believed that it is.

SLE was introduced in [22] and studied further in [21]. Expositions may be found in [12] and [24]. In the case of  $\kappa = 8/3$ , SLE satisfies the restriction property and so belongs to the one parameter family of restriction measures studied by Lawler, Schramm and Werner [14]. They showed that the probabilities of certain events for  $SLE_{8/3}$  may be computed from certain conformal maps. In some cases they may be computed explicitly. Past Monte Carlo simulations have tested the equivalence of the scaling limit of the SAW and  $SLE_{8/3}$  by computing these probabilities for the SAW by simulation and comparing with the exact result for  $SLE_{8/3}$ . Here are two examples. Let  $P$  be a point on the horizontal axis and consider the minimum distance of the  $SLE_{8/3}$  curve to the point. This is a random variable whose distribution may be computed explicitly for  $SLE_{8/3}$ . For the second example consider a vertical line given by  $x = c$  for some  $c \neq 0$ . The  $SLE_{8/3}$  curve intersects it. Let  $Y$  be the distance from the horizontal axis to the lowest intersection. The distribution of  $Y$  may be explicitly computed for  $SLE_{8/3}$ . Note that for both of these random variables the time parameterization of the curve plays no role. For these two examples and several others, excellent agreement was found between the  $SLE_{8/3}$  exact results and the simulation results for the scaling limit of the SAW [9, 10].

The SLE curve is usually parameterized so that its half-plane capacity grows linearly with the time parameter  $t$ . Before we take the scaling limit, the SAW has a natural parameterization given by the number of steps, or equivalently the distance along the curve since all steps are nearest neighbor. With a suitable scaling this should give a natural parameterization of the

scaling limit of the SAW. Equipped with these natural parameterizations, the scaling limit of the SAW and the  $\text{SLE}_{8/3}$  parameterized curves are not the same. We illustrate this with a simulation in section 2. How should these curves be reparameterized so that they agree?

There are two ways to ask this question. We can ask how to reparameterize the scaling limit of the SAW to make it agree with  $\text{SLE}_{8/3}$  with its parameterization using half-plane capacity. The answer is obvious - one should use the half-plane capacity of the scaling limit of the SAW to parameterize it. We study this in section 3.

A less obvious question is to ask how we should reparameterize  $\text{SLE}_{8/3}$  to make it agree with the scaling limit of the SAW with its natural parameterization. In section 4 we give simulation results that indicate that for the SAW with its natural parameterization, the  $p$ -variation of the walk exists and is a deterministic, linear function of time if we take  $p = 1/\nu = 4/3$ . In other words, one can recover the natural parameterization of the SAW by computing its  $1/\nu$  variation. Some care is needed here since different definitions of the variation give different values. However, it appears they differ only by a multiplicative constant. In section 5 we use the  $1/\nu$  variation of the SLE to reparameterize the SLE curve and compare this with the SAW with its natural parameterization. Section 6 discusses various computational aspects of our simulations of the SAW and the SLE.

## 2 Need for a random reparameterization

We review some facts about SLE. We refer the reader to [12] for more detail. We restrict our attention to chordal SLE in the upper half plane. It is defined by the differential equation

$$\dot{g}_t(z) = \frac{2}{g_t(z) - \sqrt{\kappa}B_t} \quad (1)$$

and the initial condition  $g_0(z) = z$ . The dot denotes differentiation with respect to time  $t$ ,  $B_t$  is a standard real-valued Brownian motion, and  $z$  belongs to the upper half plane  $\mathbb{H}$ . For some initial points  $z$ , the solution only exists for a finite time interval. The set of initial points for which the solution no longer exists at time  $t$  is a random subset  $K_t$  of  $\mathbb{H}$ . For  $\kappa \leq 4$ ,  $K_t$  is just a simple curve  $\gamma(t)$ , i.e., a curve that does not intersect itself. We use  $\gamma[0, t]$  to denote the image of the curve for the time interval  $[0, t]$ . So  $\gamma[0, t] = K_t$ .

The parameterization of the curve  $\gamma$  that results from eq. (1) corresponds to the half-plane capacity of the curve which is defined as follows. Since  $\gamma$  is simple,  $\mathbb{H} \setminus \gamma[0, t]$  is simply connected. So there is a conformal map of this domain onto  $\mathbb{H}$ . If we require the map to send  $\infty$  to itself, then this map has an expansion about  $\infty$  of the form

$$g(z) = cz + a_0 + \sum_{n=1}^{\infty} a_n z^{-n} \quad (2)$$

The map is uniquely determined if we require  $c = 1$  and  $a_0 = 0$ . The half plane capacity of  $\gamma[0, t]$  is then the coefficient  $a_1$ . We denote it by  $hcap(\gamma[0, t])$ .

The above definition applies to any simple curve  $\gamma$ . For the SLE curve we have

$$hcap(\gamma[0, t]) = 2t \tag{3}$$

If we were to parameterize SLE so that

$$hcap(\gamma[0, t]) = b(t) \tag{4}$$

for some differentiable, increasing function  $b(t)$ , then the 2 in the Schramm-Loewner equation would be replaced by  $\dot{b}(t)$ .

The scaling property of Brownian motion leads to a scaling property for SLE:  $\gamma[0, t]$  has the same distribution as  $\sqrt{t}\gamma[0, 1]$ . (Note that if we rescale a set by  $r$ , its half-plane capacity scales by a factor of  $r^2$ .) Thus

$$E[\gamma(t)^2] = ct \tag{5}$$

where  $c = E[\gamma(1)^2]$ .

The SAW has a natural parameterization. Let  $W(n)$  be the infinite SAW in the upper half plane on a lattice with unit lattice spacing. We extend  $W(t)$  to all  $t \geq 0$  by linearly interpolating between the integer times. The average distance from the origin to  $W(n)$  is believed to grow like  $n^\nu$  with  $\nu = 3/4$ . The limit of taking the lattice spacing to zero can then be obtained by defining

$$\omega(t) = \lim_{n \rightarrow \infty} n^{-\nu} W(nt) \tag{6}$$

This limit is believed to exist and give a probability measure on simple curves in the upper half plane starting at the origin, but this has not been proved. This definition of the scaling limit is analogous to Brownian motion as the scaling limit of an ordinary random walk. If we take  $W(n)$  to be an ordinary random walk in the plane and  $\nu = 1/2$ , then (6) would converge to two-dimensional Brownian motion. We refer to this parameterization of the scaling limit of the SAW as its natural parameterization. If this limit exists, then  $\omega(t)$  has the same distribution as  $t^\nu\omega(1)$ . Thus

$$E[\omega(t)^2] = bt^{2\nu} \tag{7}$$

where  $b = E[\omega(1)^2]$ .

The behavior of  $E[\gamma(t)^2]$  and  $E[\omega(t)^2]$  show that to make the scaling limit of the SAW and  $SLE_{8/3}$  agree we must at least do a deterministic reparameterization. If there is a reparameterization,  $\hat{\gamma}(t) = \gamma(\phi(t))$ , of  $SLE_{8/3}$  with a deterministic  $\phi(t)$  that makes  $\hat{\gamma}(t)$  and  $\omega(t)$  agree in distribution, then we must have  $E[\hat{\gamma}(t)^2] = E[\omega(t)^2]$  and so the reparameterization must be

$$\hat{\gamma}(t) = \gamma(at^{2\nu}) \tag{8}$$

with  $a = b/c$ .

It is easy to see from simulations that this deterministic reparameterization does not work, i.e.,  $\hat{\gamma}(t)$  and  $\omega(t)$  do not have the same distribution as parameterized curves. To show this we consider  $\hat{\gamma}(1)$  and  $\omega(1)$ . If they have the same distribution, then  $\gamma(1)/E[|\gamma(1)|]$  and

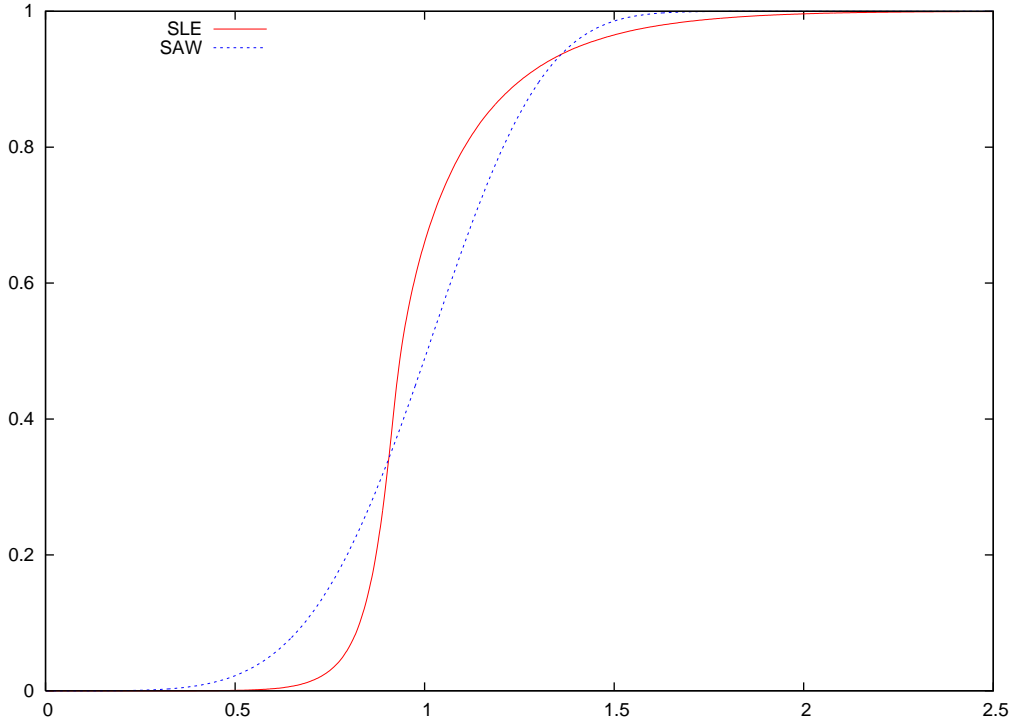


Figure 1: The distribution,  $P(R \leq t)$ , for the distance  $R$  from the origin to  $\gamma(1)$  (labeled by SLE) and to  $\omega(1)$  (labeled by SAW). Both random variables have been rescaled so that they have mean one.

$\omega(1)/E[|\omega(1)|]$  have the same distribution. For each of these two random points, we compute two random variables - the distance  $R$  from the origin to the random point and the polar angle  $\Theta$  of the random point. Our rescaling means that  $E[R] = 1$  for both the SLE and the SAW.

The distributions of  $R$  for the SLE and the SAW are shown in figure 1. The distributions of  $\Theta$  are shown in figure 2. We do not show any error bars in the figures. The width of the error bars would be hard to see on this scale. Clearly the distributions are different.

Throughout this paper our plots of the distributions of random variables are plots of their cumulative distribution functions rather than their densities. The cumulative distribution is the function that is actually computed in the simulation. Computing the density would require taking a numerical derivative.

### 3 Reparameterizing the SAW

In this section we reparameterize the scaling limit of the SAW so that it agrees with SLE with its usual parameterization. For  $t > 0$  we define  $C_t$  to be the random time for the scaling limit

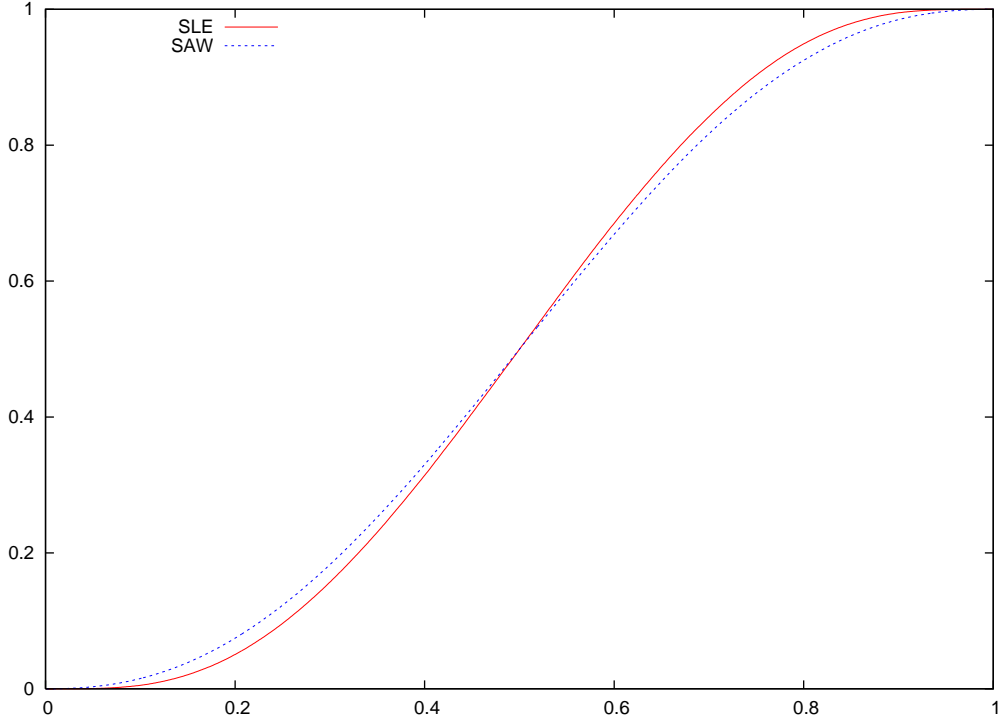


Figure 2: The distribution,  $P(\Theta \leq t)$ , for the polar angle  $\Theta$  of the points  $\hat{\gamma}(1)$  (labeled by SLE) and  $\omega(1)$  (labeled by SAW).

of the SAW when

$$hcap(\omega[0, C_t]) = 2t \tag{9}$$

We define  $\hat{\omega}(t) = \omega(C_t)$  so that  $hcap(\hat{\omega}[0, t]) = 2t$ . Then  $\hat{\omega}(t)$  and  $\gamma(t)$  should have the same distribution as parameterized curves. We test this by comparing the distributions of  $R$  and  $\Theta$  for  $\gamma(1)$  and  $\hat{\omega}(1) = \omega(C_1)$ . As before,  $R$  is the distance from the random point to the origin and  $\Theta$  is the polar angle of the random point.

If we plot the distributions of  $R$  for  $\gamma(1)$  and  $\hat{\omega}(1)$ , the two curves are virtually indistinguishable. So in figure 3 we plot the difference of these two distributions. The important thing to note about this figure is the scale on the vertical axis. The difference between the two distributions is typically on the order of a tenth of a percent. We caution the reader that in figure 1 the random variable  $R$  was rescaled so that its mean was 1. This is not done in figure 3. The mean of  $R$  here is slightly greater than 2. In particular, the sharp spikes in figure 3 just left of  $R = 2$  correspond to where the distribution is increasing sharply. In figure 1 this sharp increase occurs just left of  $R = 1$ .

The difference of the distributions of  $\Theta$  for  $\gamma(1)$  and  $\hat{\omega}(1)$  is shown in 4. Again, the most important feature of this plot is the scale on the vertical axis. These two distributions also differ by on the order of a tenth of a percent.

The error bars in figures 3 and 4 and subsequent figures are only statistical errors, i.e., the error arising from not running the Monte Carlo simulations forever. The error bars shown are two standard deviations. The standard deviation is estimated using the techniques of batched means. The simulations of the SAW and the SLE both contain systematic errors. These are discussed in section 6.

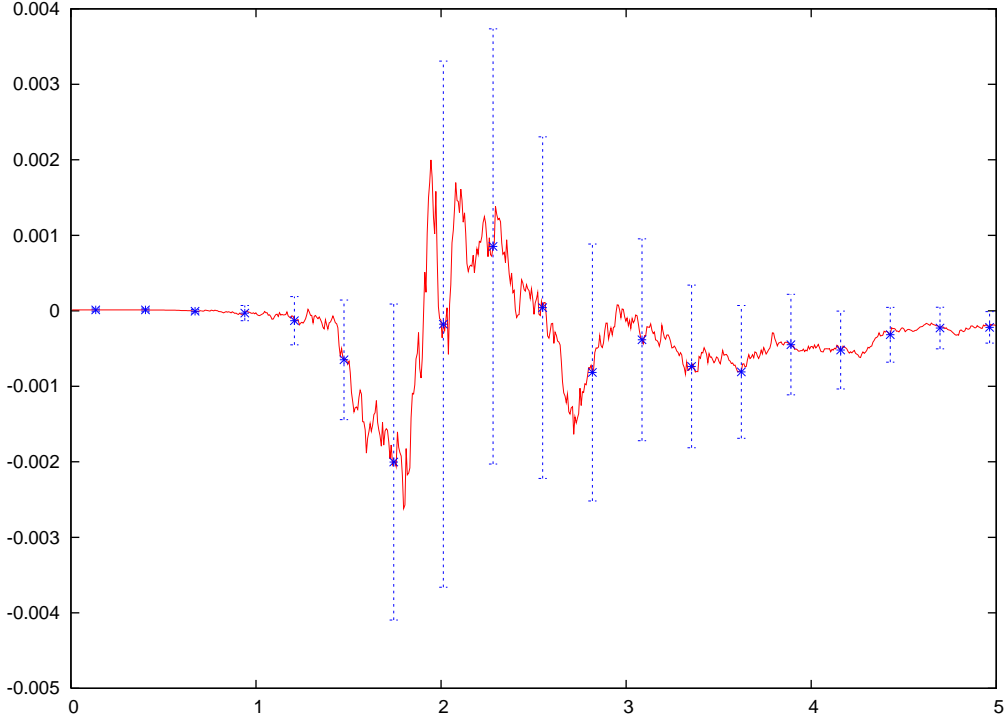


Figure 3: The difference of the distributions of  $R$  for  $\hat{\omega}(1)$ , the SAW parameterized using capacity, and  $\gamma(1)$ , the SLE with its usual parameterization.

To further test the equivalence of  $\gamma(t)$  and  $\hat{\omega}(t)$ , we consider the covariances of these two processes. We think of these processes as taking values in  $\mathbb{R}^2$  rather than the complex plane and let  $\gamma_i(t)$  and  $\hat{\omega}_i(t)$  denote their coordinates with  $i = 1, 2$ . The covariance of SLE is given by

$$C_{ij}(s, t) = E[\gamma_i(s)\gamma_j(t)] - E[\gamma_i(s)]E[\gamma_j(t)] \quad (10)$$

By scaling, the dependence of the last term on  $s$  and  $t$  is trivial:

$$E[\gamma_i(s)]E[\gamma_j(t)] = \sqrt{st}E[\gamma_i(1)]E[\gamma_j(1)] \quad (11)$$

So we will only study  $E[\gamma_i(s)\gamma_j(t)]$ . By scaling,

$$E[\gamma_i(s)\gamma_j(t)] = sE[\gamma_i(1)\gamma_j(t/s)] = tE[\gamma_i(s/t)\gamma_j(1)] \quad (12)$$

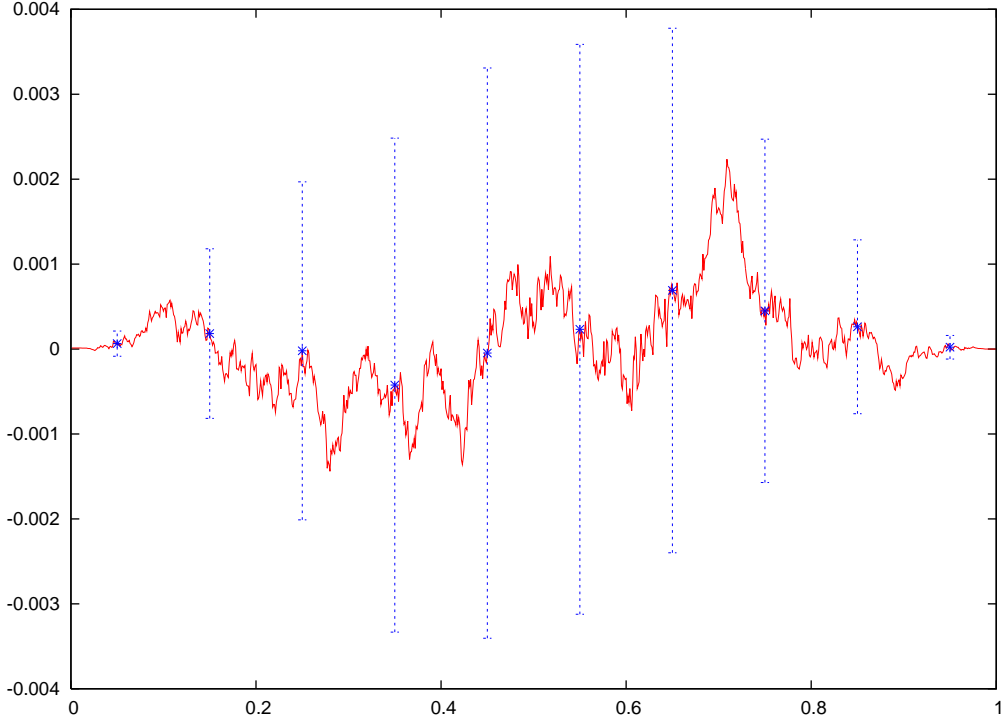


Figure 4: The difference of the distributions of  $\Theta$  for  $\hat{\omega}(1)$ , the SAW parameterized using capacity, and  $\gamma(1)$ , the SLE with its usual parameterization.

So it suffices to study this quantity with  $s = 1$  and  $0 \leq t \leq 1$ . We can rewrite this as

$$E[\gamma_i(1)\gamma_j(t)] = E[\gamma_i(t)\gamma_j(t)] + E[(\gamma_i(1) - \gamma_i(t))\gamma_j(t)] \quad (13)$$

By scaling, the first term is just  $c_{ij}t$  where  $c_{ij} = E[\gamma_i(1)\gamma_j(1)]$ . So we simulate just the second term. So let

$$\rho_{ij}(t) = E[(\gamma_i(1) - \gamma_i(t))\gamma_j(t)] \quad (14)$$

For the SAW parameterized by capacity, we define

$$\hat{\sigma}_{ij}(t) = E[(\hat{\omega}_i(1) - \hat{\omega}_i(t))\hat{\omega}_j(t)] \quad (15)$$

The functions  $\rho_{ij}(t)$  and  $\hat{\sigma}_{ij}(t)$  are shown in figure 5 for  $i = j = 1$  and  $i = j = 2$ . (It is not hard to see that by symmetry these functions are zero when  $i \neq j$ .) The functions agree so well that we have plotted individual points for  $\hat{\sigma}_{ij}(t)$  and an interpolating curve for  $\rho_{ij}(t)$  so that the two functions may be distinguished. It is much harder to simulate the SAW at a constant capacity than to simulate the SLE. Consequently the statistical errors for the SAW are larger. So we have only shown error bars for the SAW points. The difference between the covariances of SLE and the SAW parameterized by capacity is small, but appears to be greater than the



statistical error shown by the error bars in the figure. We emphasize again that these error bars do not include the systematic errors. Computing the capacity of a SAW is time consuming. This limits the SAW simulation to walks of modest length - one of the sources of systematic error.

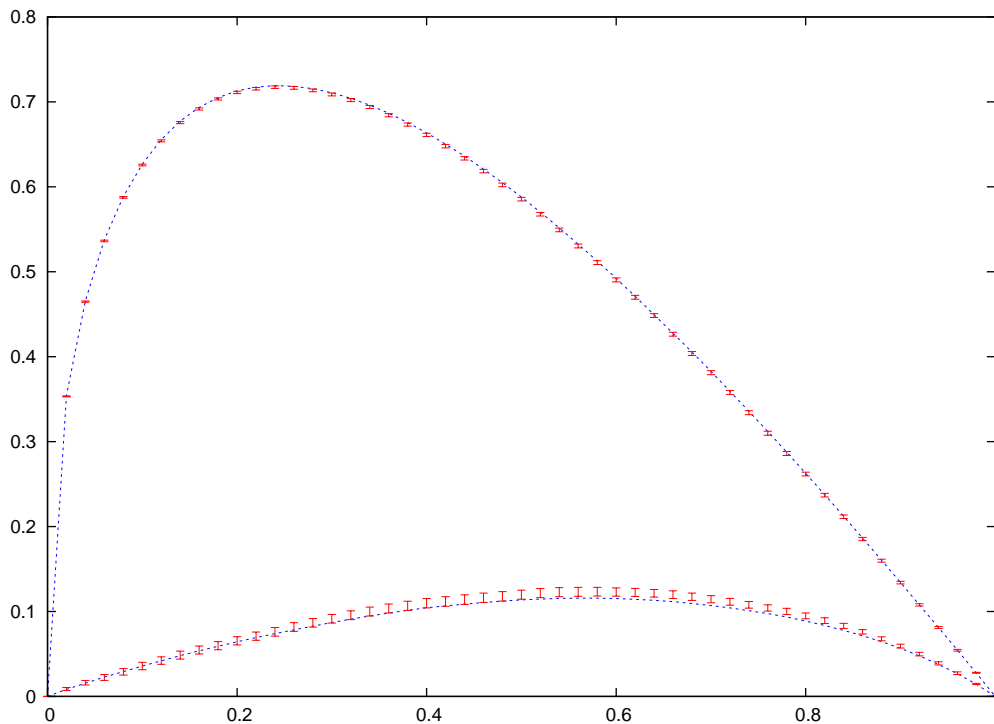


Figure 5: The covariance  $\rho_{ij}(t)$  for SLE and the covariance  $\hat{\sigma}_{ij}(t)$  for the SAW using capacity as its parameterization. The top curve is  $i = j = 2$ , the bottom curve is  $i = j = 1$ . The SLE covariance is plotted with a curve and no error bars, while individual points with error bars are plotted for the SAW.

## 4 $p$ -variation of the SAW

We now consider the question of how to reparameterize  $\text{SLE}_{8/3}$  so that it agrees with the scaling limit of the SAW with its natural parameterization. If one plots points on a SAW that are equally spaced in time, then the points appear to be equally spaced along the SAW path. In other words, the natural parameterization of the SAW corresponds to using the length of the walk as the parameter. Of course, this is only a heuristic statement since the SAW is not expected to have finite variation. However, we will see that the so called “ $p$ -variation” provides a way to make sense of the length along the SAW.

If  $X(s)$  is a stochastic process, then the  $p$ -variation is defined as follows. Let  $0 = t_0^n < t_1^n < t_2^n \cdots < t_{k_n}^n = t$  be a sequence of partitions of  $[0, t]$ . Let  $\Pi_n$  denote the  $n$ th partition and let  $|\Pi_n|$  be the width of the largest subinterval of  $\Pi_n$ . We assume that  $|\Pi_n|$  goes to zero as  $n$  goes to infinity. We define

$$var_p((X(s))_{0 \leq s \leq t}, \Pi_n) = \sum_{j=1}^{k_n} |X(t_j^n) - X(t_{j-1}^n)|^p \quad (16)$$

With some abuse of the notation we will write  $var_p((X(s))_{0 \leq s \leq t}, \Pi_n)$  as just  $var_p(X(0, t), \Pi_n)$ . We define the  $p$ -variation to be the limit as the partition gets finer:

$$var_p(X(0, t)) = \lim_{n \rightarrow \infty} var_p(X(0, t), \Pi_n) \quad (17)$$

We have not specified the nature of the convergence in the above definition, nor have we given any conditions on the sequence of partitions. In our simulations of the SAW and SLE we will use a sequence of uniform partitions for the  $\Pi_n$ . Changing the parameterization of the process is equivalent to changing the partitions used. As we will see, changing the parameterization can change the value of the  $p$ -variation.

It is important to note that we do not take a supremum over all partitions in the definition of the  $p$ -variation. If one takes a supremum one obtains a different quantity which, unfortunately, is also called the  $p$ -variation in the literature. (It is sometimes called the strong  $p$ -variation.) For Brownian motion and  $p = 2$  the variation we have defined is the quadratic variation studied by Lévy [16]. If the sequence of partitions satisfies  $|\Pi_n| = o(1/\log(n))$ , then the quadratic variation of Brownian motion converges with probability one to  $t$  [4]. But if the condition is relaxed to  $|\Pi_n| = O(1/\log(n))$  this is not true [5]. For other values of  $p$ , the  $p$ -variation has been shown to exist for certain Gaussian processes including fractional Brownian motion and the local times associated with a symmetric stable Lévy process. See the recent references [6, 18, 19, 23] and references therein.

Now consider the SAW. If the scaling limit exists then  $|\omega(t_j) - \omega(t_{j-1})|$  is of size  $(t_j - t_{j-1})^\nu$ . So it is natural to consider the  $p$ -variation with  $p = 1/\nu$ . We conjecture that

$$var_{1/\nu}(\omega(0, t)) = ct \quad (18)$$

for some constant  $c$ . If the  $1/\nu$  variation exists for the scaling limit of the SAW, then it is trivial to see that

$$E[var_{1/\nu}(\omega(0, t))] = ct \quad (19)$$

for some constant  $c$ . So the content of the conjecture is that the  $1/\nu$  variation exists and is non-random. For the remainder of the paper,  $p$  will be  $1/\nu = 4/3$ , and so we will drop the subscript  $1/\nu$  on  $var$ .

We support the conjecture with a simulation. We only consider a uniform partition with intervals of width  $\Delta t$ , and we take  $t = 1$ . In this case we denote  $var(\omega(0, 1), \Pi)$  by  $var(\omega(0, 1), \Delta t)$ .

The distribution of this random variable is shown in figure 6 for several values of  $\Delta t$ . Two different sets of curves are shown in this figure. The curves on the right side of the figure are for the variation defined above. Note that the scale on the horizontal axis begins at 0.92, not 0. The figure clearly indicates that the distribution is converging to a step function as it should if the  $1/\nu$  variation is constant.

To study the convergence quantitatively, in figure 7 we plot the variance of the random variable  $var(\omega(0, 1), \Delta t)$  as a function of  $\Delta t$ . Three curves are shown in this figure. The variance of  $var(\omega(0, 1), \Delta t)$  is the line of points labeled “var.” In this log-log plot the data is very well fit by a line with slope 1. This corresponds to the variance being proportional to  $\Delta t$ . Note that this is what we would find if the process had independent, stationary increments. We do not expect the increments of the SAW to be independent, but this result suggests that the lengths of these increments are weakly correlated.

The fractional variation defined above involves the parameterization of the SAW. A different parameterization could give a different value to this variation. (We will see an example of this later.) Another definition of the variation that does not depend on the parameterization is the following. Let  $\Delta t > 0$ . We define times  $t_i$  as follows.  $t_0 = 0$ . Given  $t_i$ , we let  $t_{i+1}$  be the first time after  $t_i$  such that  $|\omega(t_{i+1}) - \omega(t_i)| = (\Delta t)^\nu$ . The variation over the time interval  $[0, t]$  is then defined to be  $n\Delta t$ , where  $n$  is the largest index with  $t_n \leq t$ . We denote this variation by  $var_{no}(\omega(0, t), \Delta t)$ . The subscript *no* stands for “no parameterization,” to emphasize that this definition does not depend on how the curve is parameterized.

The curves on the left of figure 6 show the variation  $var_{no}(\omega(0, 1), \Delta t)$  for several values of  $\Delta t$ . The figure shows this variation is also converging to a constant. It also shows that the constant  $var_{no}(\omega[0, t])$  is slightly less than the constant  $var(\omega[0, t])$ . The variance of  $var_{no}(\omega[0, t], \Delta t)$  is the line of points labeled “var<sub>no</sub>” in figure 7. This data is also very well fit by a line with slope 1.

We now return to our first definition of the  $p$ -variation, eq. (16), and consider what can happen if we use a different parameterization. We are particularly interested in what happens when we use the half-plane capacity to reparameterize the SAW. We denote the resulting variation by  $var_{cap}(\omega(0, t), \Pi_n)$ . We can numerically compute the capacity along a SAW and so we can simulate this random variable. We have simulated it with a uniform partition. Computing the capacity is difficult and this limits the lengths of the SAW’s we can study. This in turn restricts the simulations to larger values of  $\Delta t$ . The distributions of this random variable for several choices of  $\Delta t$  are shown in figure 8. The first thing to note about this figure is the scale on the horizontal axis. These distributions have considerably larger variance than the curves in figure 6 with the same values of  $\Delta t$ . Nonetheless, it appears this this random variable is also converging to a constant as  $\Delta t$  goes to zero. We also see that  $var_{cap}(\omega(0, 1))$  is slightly less than  $var_{no}(\omega(0, 1))$ . The variance of  $var_{cap}(\omega(0, 1), \Delta t)$  as a function of  $\Delta t$  is the set of points labeled “var<sub>cap</sub>” in figure 7. This data indicates the variance is converging to zero as  $\Delta t$  goes to zero, but it is not well fit by any line, at least for the range of  $\Delta t$  shown.

For each of the three variations we have studied, the plots of their distributions for three values of  $\Delta t$  very nearly have a common point of intersection. This provides a simple way to

estimate the values of these variations in the limit  $\Delta t \rightarrow 0$ . We estimate

$$\begin{aligned}
 \text{var}(\omega(0, 1)) &= 0.987 \pm 0.001 \\
 \text{var}_{no}(\omega(0, 1)) &= 0.972 \pm 0.001 \\
 \text{var}_{cap}(\omega(0, 1)) &= 0.92 \pm 0.01
 \end{aligned}
 \tag{20}$$

The error bars we have given are just guesses. As we discuss in section 6 there are systematic errors in the simulations which make it difficult to give reliable error bars.

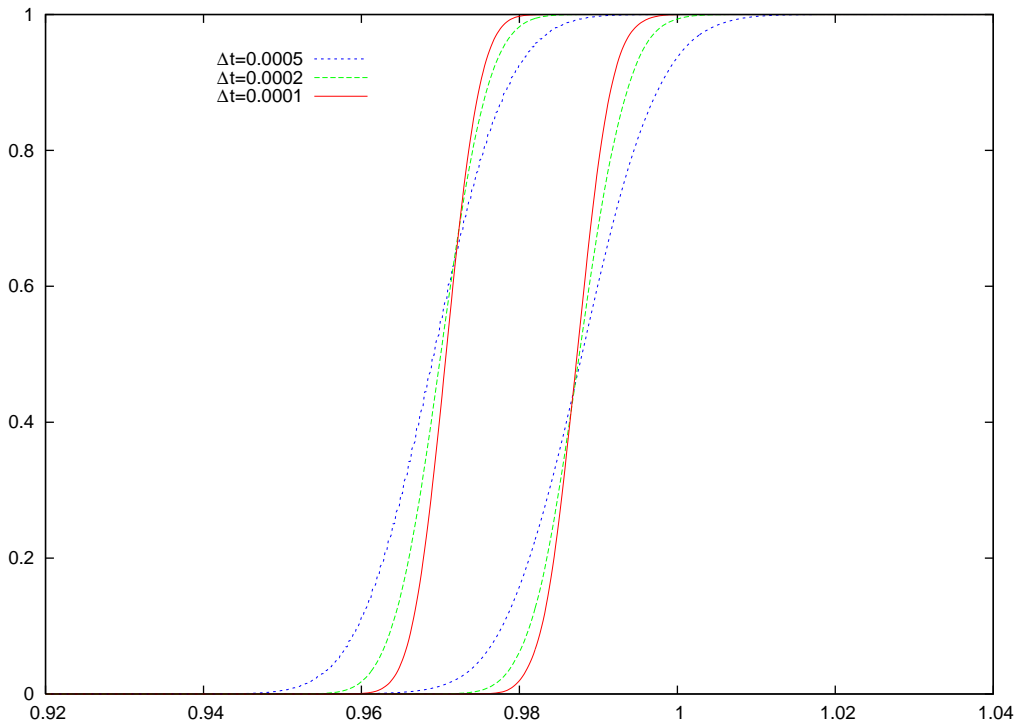


Figure 6: The set of curves on the right are the distributions of  $\text{var}(\omega(0, 1), \Delta t)$ ; those on the left are the distributions of  $\text{var}_{no}(\omega(0, 1), \Delta t)$ .

## 5 Reparameterizing the SLE

If the scaling limit of the SAW is indeed SLE, then the results of the previous section suggest that each of the  $1/\nu$  variations we considered should exist for SLE and give a parameterization which corresponds to the natural parameterization of the SAW. Of course, there is no way to compute the variation  $\text{var}(\omega[0, t])$  for SLE since it requires knowing the parameterization we

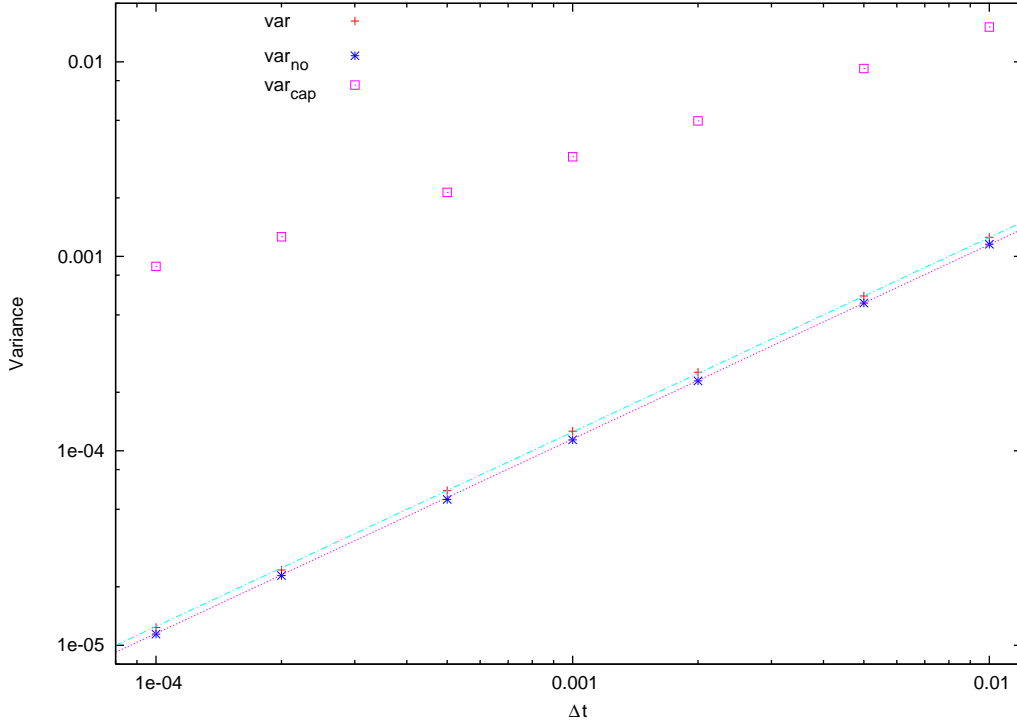


Figure 7: The variance of the three different definitions of the  $p$ -variation as functions of  $\Delta t$ .

are trying to find. We must either use  $var_{no}(\omega[0, t])$  or  $var_{cap}(\omega[0, t])$ . We use the former since its variance for a nonzero  $\Delta t$  is smaller. Let  $V_t$  be the random time on the SLE where

$$var_{no}(\gamma[0, V_t]) = ct \quad (21)$$

where  $c = var_{no}(\omega[0, 1])$ . We define  $\hat{\gamma}(t) = \gamma(V_t)$  so that  $var_{no}(\hat{\gamma}[0, t]) = var_{no}(\omega[0, t])$ . Then  $\hat{\gamma}(t)$  and  $\omega(t)$  should have the same distribution as parameterized curves. We test this by comparing the distributions of  $\omega(1)$  and  $\hat{\gamma}(1) = \gamma(V_1)$ .

We must compute the constant  $c = var_{no}(\omega[0, 1])$  by simulation. This requires computing the variation  $var_{no}(\omega(0, 1), \Delta t)$  for several  $\Delta t$  and then estimating the limit as  $\Delta t \rightarrow 0$ . However, when we compute the variation  $var_{no}(\gamma[0, V_t])$  we must also use a nonzero  $\Delta t$  and then attempt to take a limit as  $\Delta t \rightarrow 0$ . These extrapolations have some error in them. We attempt to minimize this error by the following trick. For a given  $\Delta t$  we define  $V_t$  by

$$var_{no}(\gamma[0, V_t], \Delta t) = var_{no}(\omega[0, 1], \Delta t) t \quad (22)$$

and then let  $\hat{\gamma}(t) = \gamma(V_t)$ . In other words, for the constant  $c$  we use the estimate of  $c$  that comes from the SAW simulation using the same value of  $\Delta t$  that we use to compute the  $p$ -variation for the SLE. (Note that  $V_t$  now has some small dependence on  $\Delta t$ .)

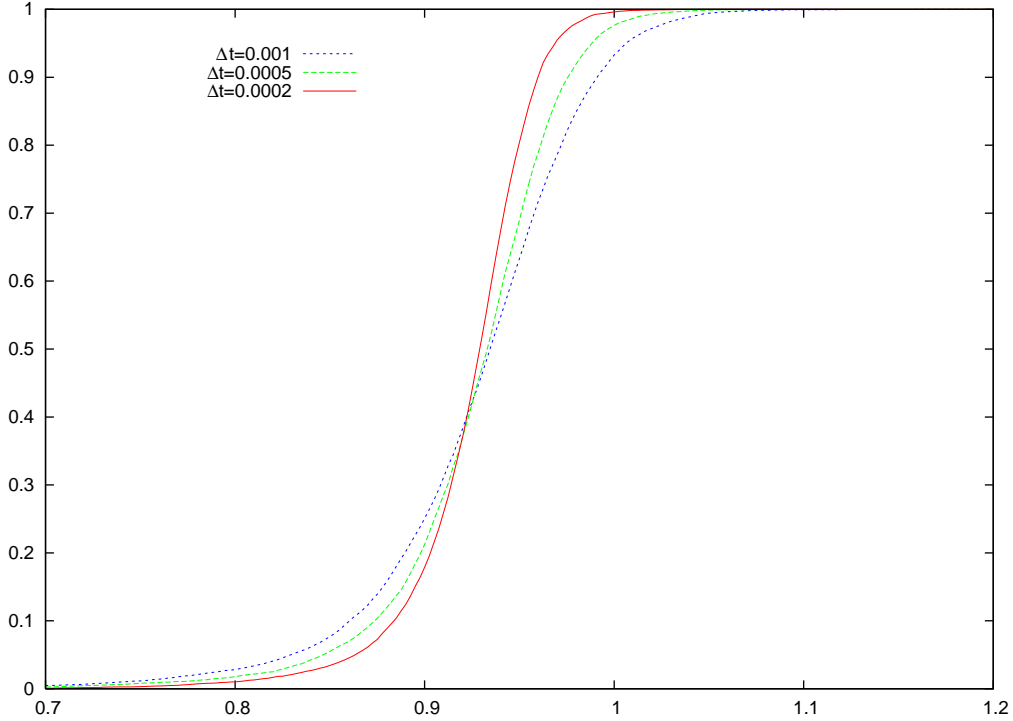


Figure 8: The distribution of  $\text{var}_{\text{cap}}(\omega(0,1), \Delta t)$ , the random variable that converges to the  $p$ -variation computed using the parameterization of the SAW by capacity.

As before we compute the distributions of the random variables  $R$  and  $\Theta$ . In figure 9 we show the difference between the distributions of  $R$  for  $\omega(1)$  and  $\hat{\gamma}(1)$ . Two plots are shown corresponding to two different values of  $\Delta t$ . The difference is larger than that seen in figure 3. However, the figure also shows that the difference depends strongly on  $\Delta t$ . In figure 10 we show the difference between the distributions of  $\Theta$  for  $\omega(1)$  and  $\hat{\gamma}(1)$ . For the angle we see almost no dependence on the choice of  $\Delta t$ .

Next we test the equivalence of  $\hat{\gamma}(t)$  and  $\omega(t)$  by comparing their covariances. As we saw before, the non-trivial part of these covariances is given by

$$\hat{\rho}_{ij}(t) = E [(\hat{\gamma}_i(1) - \hat{\gamma}_i(t))\hat{\gamma}_j(t)] \quad (23)$$

and

$$\sigma_{ij}(t) = E [(\omega_i(1) - \omega_i(t))\omega_j(t)] \quad (24)$$

These functions are shown in figure 11 for  $i = j = 1$  and  $i = j = 2$ . The SAW and SLE covariances agree reasonably well. As in figure 9 there is significant dependence on the  $\Delta t$  used to compute the  $p$ -variation of the SLE. For some values of  $\Delta t$  the agreement between the two covariances is not as good as that shown in the figure.

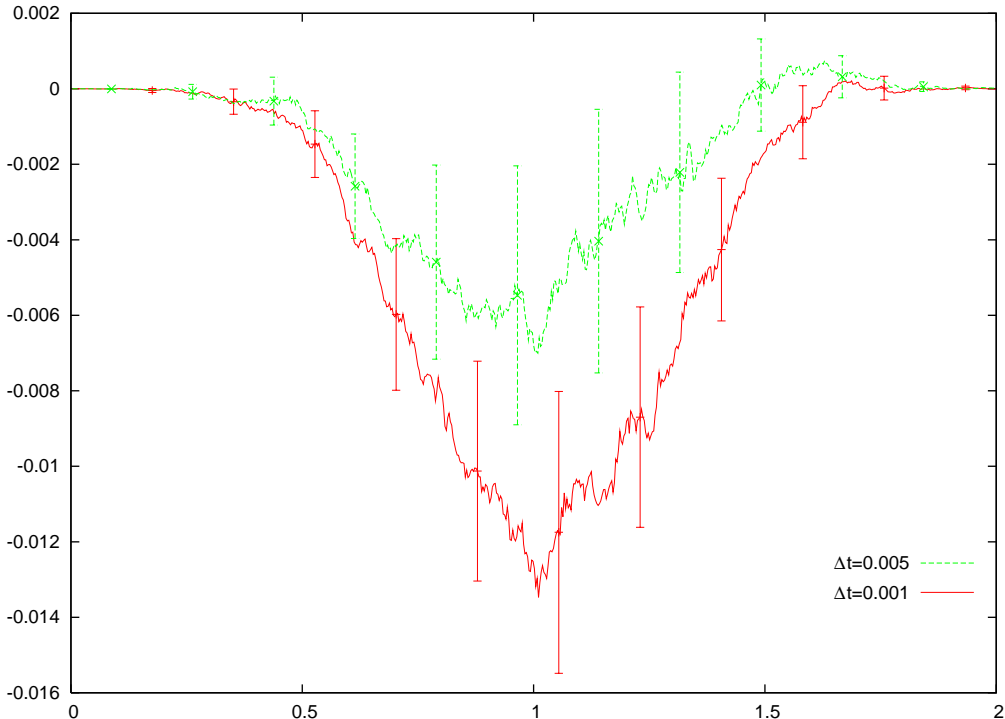


Figure 9: The difference of the distributions of  $R$  for  $\omega(1)$ , the SAW with its natural parameterization, and  $\hat{\gamma}(1)$ , the SLE parameterized by the variation  $var_{no}$ .

It is tempting to compare the plots in figures 5 and 11. The first thing to keep in mind is that in figure 5,  $t = 1$  corresponds to  $hcap = 2$  while in figure 11,  $t = 1$  corresponds to  $var_{no} = 1$ . Simulations show that the average capacity for a SAW with  $var_{no} = 1$  is close to 0.5. Changing the capacity by a factor of 4 is the same as changing spatial scales by a factor of 2, and so corresponds to a change in the covariance by a factor of 4. Indeed the vertical scales in the two figures differ by a factor of approximately 4. However, we should emphasize that the two plots use completely different parameterizations of the processes and so comparing them is not particularly meaningful. These two plots should be different even if they are rescaled to have the same vertical scale.

## 6 Simulating SAW and SLE

One method for simulating SLE is to approximate the conformal map  $g_t$  by the composition of a large number of conformal maps which are known explicitly. A particular implementation was studied by R. Bauer [1]. This method is also briefly discussed for the radial case in [20]. Here we give a brief overview. A more detailed review may be found in [7].

We consider the time interval  $[0, 1]$  and divide it into  $N$  subintervals. (We could use a

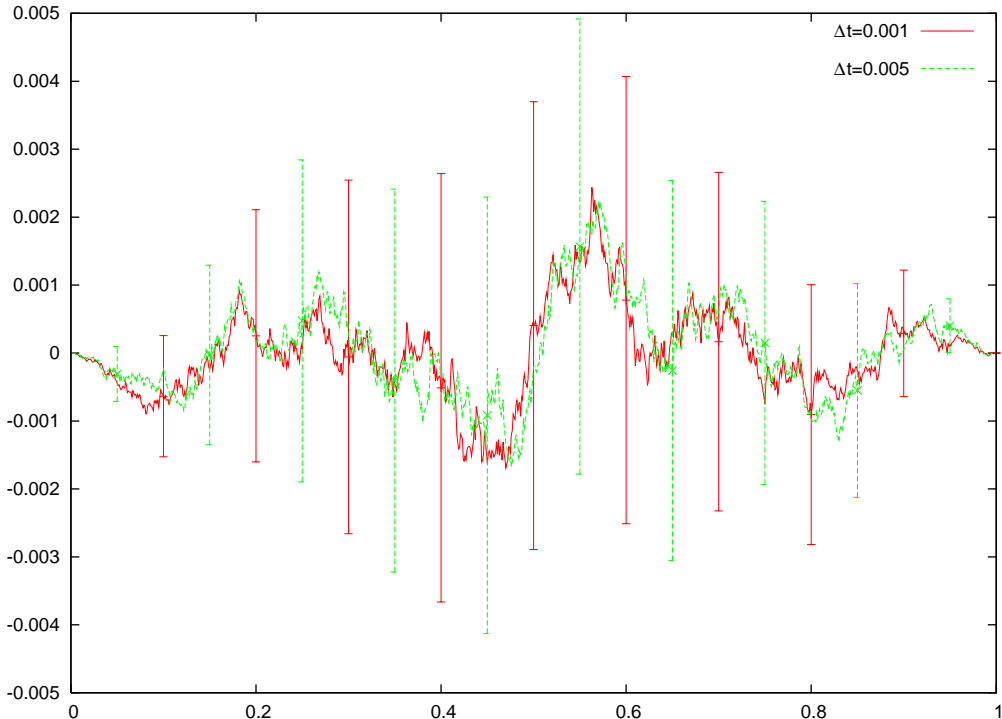


Figure 10: The difference of the distributions of  $\Theta$  for  $\omega(1)$ , the SAW with its natural parameterization, and  $\hat{\gamma}(1)$ , the SLE parameterized by the variation  $var_{no}$ .

uniform partition of  $[0, 1]$ , but one obtains a more uniform distribution of points along the SLE curve by using a non-uniform partition of the time interval. See [7] for details.) The conformal map  $g_t$  can be written as the composition of  $N$  conformal maps, each of which corresponds to the solution of the SLE equation (1) over one of the small time intervals. Each of these  $N$  conformal maps is approximated by a simple conformal map. We use the conformal map that takes the half plane minus a slit onto the half plane. The parameters for these conformal maps (e.g., the length and angle of the slit) are chosen so that the conformal maps have the correct capacity and so that the driving function corresponding to the composition of these conformal maps approximates the original driving function  $\sqrt{\kappa}B_t$ . For example, this can be done so that the driving function of the approximation agrees with  $\sqrt{\kappa}B_t$  at the times which are endpoints of the  $N$  subintervals.

To compute a point on the SLE trace, one must apply  $O(N)$  of these conformal maps. So the time to compute a single point is  $O(N)$ . If one wants to compute  $N$  points on the SLE trace this will take a time  $O(N^2)$ . The paper [7] shows how to implement this method of simulating the SLE so that the time required to compute a single point is approximately  $O(N^{0.4})$  rather than  $O(N)$ .

Certain features of the SLE are relatively easy to study by simulation. For example, to



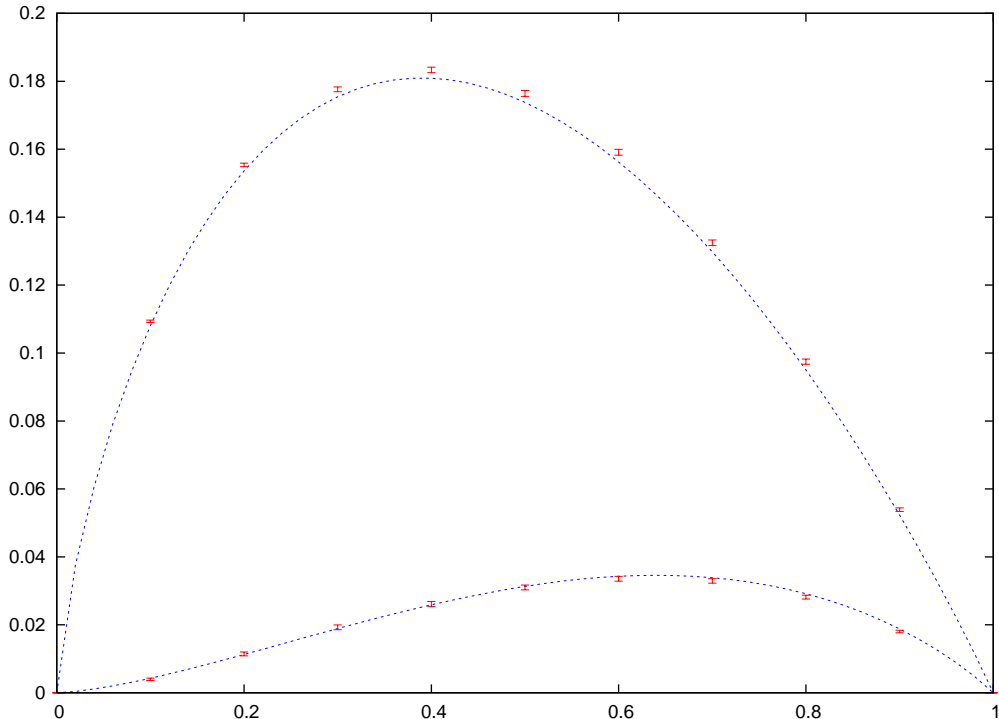


Figure 11: The covariance  $\sigma_{ij}(t)$  for the SAW and the covariance  $\hat{\rho}_{ij}(t)$  for SLE using the variation  $var_{no}$  for its parameterization. The top curve is  $i = j = 2$ , the bottom curve is  $i = j = 1$ . The SLE covariance is plotted with a curve and no error bars, while individual points with error bars are plotted for the SAW.

compute the distribution of the SLE trace at a fixed time, one need only compute a single point on the SLE trace. One can use a relatively large value of  $N$  and generate a large number of samples. By contrast, computing the  $1/\nu$  variation of the curve involves a double limit. One needs to let  $N \rightarrow \infty$  and then let the time interval,  $\Delta t$ , used to compute the variation go to zero. In practice this means that one must take a small  $\Delta t$  and then take  $N$  large enough that  $1/N$  is small compared to  $\Delta t$ . Thus the simulations that require computing the variation are among the most difficult.

We simulate the SAW using the pivot algorithm [17]. The particular implementation of the pivot algorithm we use is found in [8]. This algorithm is fast in two dimensions, and one can study quantities like the location of the SAW at a fixed time for walks with a million steps. The difficult part of the SAW simulations is computing the capacity of a walk. This can only be done for much shorter walks.

We compute the capacity of a SAW using the zipper algorithm [11, 20]. We give a brief explanation of how the algorithm works in our context and refer the reader to [20] for more detail. Consider a curve  $\omega(t)$  in the upper half plane which starts at the origin and ends at

$P$ , e.g., a self-avoiding walk. To compute the capacity we need to find the conformal map  $g(z)$  that takes the half plane  $\mathbb{H}$  minus the curve onto  $\mathbb{H}$ . It should be normalized so that  $g(\infty) = \infty$  and  $g'(\infty) = \infty$ . This determines the map up to a translation. The capacity is the coefficient of  $1/z$  in the expansion of  $g(z)$  about  $\infty$ . It does not depend on the choice of translation.

Let  $0 = z_0, z_1, z_2, \dots, z_n = P$  be points along the curve. Let  $C_i$  denote the portion of the curve from  $z_{i-1}$  to  $z_i$ . Let  $g_1(z)$  be the conformal map that takes  $\mathbb{H} \setminus C_1$  onto  $\mathbb{H}$ . In addition to the above normalizations, we require  $g_1(z_1) = 0$ . Then  $g_1$  maps  $C_2 \cup \dots \cup C_n$  to a curve that starts at  $0 = g_1(z_1)$  and ends at  $g_1(z_n)$  and passes through the points  $g_1(z_i)$ ,  $i = 2, \dots, n-1$ . Now we let  $g_2(z)$  be the conformal map that takes  $\mathbb{H} \setminus g_1(C_2)$  onto  $\mathbb{H}$ . Then  $g_2 \circ g_1(z)$  takes  $C_3 \cup \dots \cup C_n$  to a curve that starts at  $0 = g_2 \circ g_1(z_2)$ , ends at  $g_2 \circ g_1(z_n)$  and passes through the points  $g_2 \circ g_1(z_i)$ ,  $i = 3, \dots, n-1$ . We continue to remove one  $C_i$  at a time.  $g_i(z)$  is the conformal map that takes  $\mathbb{H} \setminus g_{i-1} \circ \dots \circ g_2 \circ g_1(C_i)$  onto  $\mathbb{H}$ . The composition  $g(z) = g_n \circ \dots \circ g_2 \circ g_1(z)$  is then the desired conformal map. The capacity of  $g$  is the sum of the capacities of the  $g_i$ .

Note that even if the original curve is piece-wise linear, the segments of the form  $g_1(C_1)$ ,  $g_2 \circ g_1(C_2) \dots$  are not. The key idea of the zipper algorithm is to approximate  $g_i$  by the conformal map  $h_i$  that takes  $\mathbb{H} \setminus D_i$  onto  $\mathbb{H}$  where  $D_i$  is a curve that starts at 0 and ends at  $g_{i-1} \circ \dots \circ g_2 \circ g_1(z_i)$ . So  $D_i$  has the same endpoints as  $g_{i-1} \circ \dots \circ g_2 \circ g_1(C_i)$ . The curve  $D_i$  is chosen so that the map  $h_i$  is relatively easy to compute. One possibility is to take  $D_i$  to be a line segment from 0 to  $g_{i-1} \circ \dots \circ g_2 \circ g_1(z_i)$ . Then there is an explicit expression for the inverse of  $h_i$  and  $h_i$  itself may be found by a Newton's method. (Some care is needed in implementing Newton's method [20].) Another choice is to take  $D_i$  to be the arc of the circle that is perpendicular to the real axis and connects 0 and  $g_{i-1} \circ \dots \circ g_2 \circ g_1(z_i)$ . This has the advantage that  $h_i$  only involves linear fractional transformations and a square root.

Because of the need to compute  $g_{i-1} \circ \dots \circ g_2 \circ g_1(z_i)$  for every point  $z_i$ , the zipper algorithm requires a time  $O(n^2)$ . The idea in [7] that speeds up the SLE simulation may be applied here to dramatically reduce the time required by this algorithm.

The curve  $D_i$  starts and ends at the same points as  $g_{i-1} \circ \dots \circ g_2 \circ g_1(C_i)$ , but does not necessarily approximate it well. For a fixed curve one improves the approximation to the capacity by using more points  $z_1, \dots, z_n$  along the curve. We do not do this. Thus the capacity we compute is not exactly the capacity of the SAW. However, it is the exact capacity (up to numerical errors) of some curve that passes through the same lattice points as the SAW. We expect that this curve will have the same scaling limit as the SAW.

As in any Monte Carlo simulation there is error because we do not run the simulation forever. We refer to this as "statistical error." It is relatively easy to estimate (we use batched means). There are also systematic errors in the simulations which we now discuss.

For the SAW, the scaling limit is given by a double limit. First we should let the length of the walk go to infinity and then take the lattice spacing to zero. In practice we fix a large  $N$  and simulate SAW's with  $N$  steps but only use the first  $N'$  steps where  $N'$  is significantly smaller than  $N$ . The simulation is done with a unit lattice, but then we rescale the walks by a factor of  $(N')^{-\nu}$ . So the portion of the rescaled SAW that we use has a size of order 1 and approximates the scaling limit of the SAW with the natural parameterization running from

$t = 0$  to  $t = 1$ . For the SAW simulations we will give the number of iterations of the Monte Carlo Markov Chain. This number is typically very large, but the samples generated are highly correlated.

For the SLE,  $N$  denotes the number of conformal maps used in the approximation. For the SLE simulations we will give the number of SLE's generated. These samples are independent.

We end this section with a discussion of the parameters used in the various simulations. In figures 1 and 2, the SAW is simulated using  $N = 1,000,000$  and  $N' = 200,000$ . The simulation ran for 1 billion iterations. The SLE simulation used  $N = 100,000$ , and 1 million samples were generated. These large numbers are possible because all we need to compute for the SLE is the location of its position at  $t = 1$ .

In figures 3 and 4 the SLE simulation used is the same as that in figures 1 and 2. The SAW simulation requires computing the capacity of the walk. This limits the simulation to significantly shorter walks. We take  $N = 100,000$  and rescale the walk by a factor of  $N^{-\nu}$ . For this rescaled walk we compute the capacity along the walk up until  $hcap = 0.1$ . (The number of steps at which this occurs is random but well below  $N$ . The mean number of steps at which the capacity is 0.1 is about a third of the total number of steps.) We then rescale the SAW again by a factor of  $\sqrt{20}$  so that the random time we are finding is where the capacity is 2. As we have noted the samples generated by the SAW simulation are highly correlated. If we are studying an observable which is trivial to compute, we might as well compute the value of the observable at every time step. The samples will be highly correlated, but there is very little cost in terms of computation time. For observables that are not trivial to compute, e.g., observables that involve computing the capacity, if we computed the observable at every time step we would spend most of the computation time on computing the observable. For such observables we only compute it every  $s$  time steps. In this SAW simulation we took  $s = 100,000$ . The simulation was run for 8 billion iterations, so 80,000 samples of the observables were computed.

For the first covariance plot, figure 5, the SLE simulation is done with  $N = 10,000$ . We compute the SLE covariance at 50 equally spaced times. 200,000 samples of the SLE were generated. For the SAW simulation, we take  $N = 100,000$ , rescale the walk by a factor of  $N^{-\nu}$ , and then compute the capacity along the walk up until  $hcap = 0.1$ . We then rescale the SAW again by a factor of  $\sqrt{20}$  so that the random time we are finding is where the capacity is 2. Computing the capacity of the SAW is slow, so we only compute it every 100,000 iterations of the Markov chain. We ran the chain for 8 billion iterations, so we generated 80,000 samples of the SAW covariance.

There are two simulations of the SAW in figure 6. In both of them  $N = 1,000,000$  and we use  $N' = 500,000$  and  $N' = 1,000,000$ . For most observables, taking  $N'$  at or near  $N$  is a bad idea - it will change the distribution of the observable. However, for the two variations shown in the figure we find no difference between the variations computed using  $N' = 500,000$  and  $N' = 1,000,000$ . The curves shown use the latter value. Both simulations were run for 1 billion iterations.

In the simulation of the SAW used for figure 8, we take  $N = 100,000$  and  $N' = 10,000$ . The relatively small value of  $N'$  is because of the difficulty in computing the capacity of a SAW. We

run the Markov chain for 1 billion iterations, but only compute  $var_{cap}$  every 100,000 iterations for a total of only 10,000 samples.

In figures 9 and 10 the SAW simulation used is the same as that in figures 1 and 2. For the SLE simulation we took  $N = 500,000$ . However, we only computed every fifth point along the SLE, so we compute a total of 100,000 points on the SLE. We generated 146,000 samples. This is the longest simulation in this paper. It required approximately 150 cpu-days. The time needed for this simulation is significantly reduced by the following trick. We compute the variation  $var_{no}$  up to the time when it is 1. This time on the SLE when this is attained is random, but occurs well before the end of the SLE we are computing. So we actually only need to compute some initial fraction of the 100,000 points on the SLE.

Finally, for figure 11 the SAW simulation uses  $N = 1,000,000$  and  $N' = 400,000$ . The SAW simulation was run for 1 billion iterations. For the SLE simulation,  $N = 250,000$  but only every fifth point was computed. Again, as discussed in the preceding paragraph we need only compute an initial portion of the SLE. 127,000 samples of the SLE were generated.

## 7 Conclusions

The main conclusion of this paper is that the  $p$ -variation with  $p = 1/\nu$  of the SLE trace provides a parameterization that corresponds to the natural parameterization of the SAW. Simulations show that the  $p$ -variation of the SAW is non-random. A trivial scaling argument then implies it is proportional to the natural parameterization of the SAW. Thus the SLE with the  $p$ -variation as its parameterization and the SAW with its natural parameterization should agree as parameterized curves. Two tests were done to check this agreement. The distributions of the random curves at a fixed time were compared, and the covariances of the two processes were compared. Good agreement was found.

A secondary conclusion of this paper concerns using the half-plane capacity to reparameterize the SAW. With this reparameterization it should agree with the SLE as parameterized curves. The same two tests of their equivalence as parameterized curves showed good agreement.

For random fractal curves like the SAW or the loop-erased random walk the exponent  $\nu$  should be equal to the reciprocal of the Hausdorff dimension of the curve. Beffara [2, 3] has proved that if  $\gamma$  is the SLE trace with parameter  $\kappa$ , then the Hausdorff dimension of  $\gamma$  is  $1 + \kappa/8$  a.s. This suggests that the  $p$ -variation of SLE should exist for  $p = \nu^{-1} = 1 + \kappa/8$ . A natural question is to consider this variation for other discrete models and see if it exists and is non-random as it appears to be for the SAW. Preliminary simulations of the loop-erased random walk indicate that its  $1/\nu$  variation exists and is non random for  $\nu = 4/5$ . This was one of the models considered by Schramm in his original paper [22]. Lawler, Schramm and Werner [15] have proved that its scaling limit converges to SLE with  $\kappa = 2$ .

**Acknowledgments:** The Banff International Research Station made possible many useful

interactions. In particular, the author thanks David Brydges, Greg Lawler, Don Marshall, Daniel Meyer, Yuval Peres, Stephen Rohde, Oded Schramm, Wendelin Werner and Peter Young for useful discussions. This work was supported by the National Science Foundation (DMS-0201566 and DMS-0501168).

## References

- [1] R. Bauer, Discrete Loewner evolution, preprint. Archived as math.PR/0303119 in arXiv.org.
- [2] V. Beffara, Hausdorff dimensions for  $SLE_6$ , *Ann. Probab.* **32**, 2606–2629 (2004). Archived as math.PR/0204208 in arXiv.org.
- [3] V. Beffara, The dimension of the SLE curves, preprint. Archived as math.PR/0211322 in arXiv.org.
- [4] R. .M. Dudley, Sample functions of the Gaussian process, *Ann. Probab.* **1**, 66–103 (1973).
- [5] W. Fernández de la Vega, On almost sure convergence of quadratic Brownian variation, *Ann. Probab.* **2**, 551–552 (1974).
- [6] P. J. Fitzsimmons and R. K. Gettoor, Limit theorems and variation properties for fractional derivatives of the local time of a stable process, *Ann. Inst. Henri Poincaré* **28**, 311–333 (1992).
- [7] T. Kennedy, A fast algorithm for simulating the chordal Schramm-Loewner evolution, preprint. Archived as math.PR/0508002 in arXiv.org.
- [8] T. Kennedy, A faster implementation of the pivot algorithm for self-avoiding walks, *J. Stat. Phys.* **106**, 407–429 (2002). Archived as cond-mat/0109308 in arXiv.org.
- [9] T. Kennedy, Monte Carlo Tests of Stochastic Loewner Evolution Predictions for the 2D Self-Avoiding Walk, *Phys. Rev. Lett.* **88**, 130601 (2002). Archived as math.PR/0112246 in arXiv.org.
- [10] T. Kennedy, Conformal invariance and stochastic Loewner evolution predictions for the 2D self-avoiding walk - Monte Carlo tests, *J. Stat. Phys.* **114**, 51–78 (2004). Archived as math.PR/0207231 in arXiv.org.

- [11] R. Kühnau, Numerische Realisierung konformer Abbildungen durch "Interpolation", *Z. Angew. Math. Mech.* **63**, 631-637 (1983).
- [12] G. Lawler, *Conformally Invariant Processes in the Plane*, *Mathematical Surveys and Monographs*, vol. 114, American Mathematical Society, 2005.
- [13] G. Lawler, O. Schramm, W. Werner, On the scaling limit of planar self-avoiding walk, *Fractal Geometry and Applications: a Jubilee of Benoit Mandelbrot, Part 2*, 339–364, *Proc. Sympos. Pure Math.* 72, Amer. Math. Soc., Providence, RI, 2004. Archived as math.PR/0204277 in arXiv.org.
- [14] G. Lawler, O. Schramm, W. Werner, Conformal restriction: the chordal case, *J. Amer. Math. Soc.* **16**, 917-955 (2003). Archived as math.PR/0209343 in arXiv.org.
- [15] G. Lawler, O. Schramm, W. Werner, Conformal invariance of planar loop-erased random walks and uniform spanning trees, *Ann. Probab.* **32**, 939–995 (2004). Archived as math.PR/0112234 in arXiv.org.
- [16] P. Lévy, Le mouvement brownien plan, *Amer. J. Math.* **62**, 487–550 (1940).
- [17] N. Madras and G. Slade, *The Self-Avoiding Walk*, Birkhäuser, Boston-Basel-Berlin, 1993.
- [18] M. B. Marcus and J. Rosen, Sample path properties of the local times of strongly symmetric Markov processes via Gaussian processes, *Ann. Probab.* **20**, 1603–1684 (1992).
- [19] M. B. Marcus and J. Rosen,  $p$ -variation of the local times of symmetric stable processes and of Gaussian processes with stationary increments, *Ann. Probab.* **20**, 1685–1713 (1992).
- [20] D. E. Marshall and S. Rohde, Convergence of the Zipper algorithm for conformal mapping, preprint.
- [21] S. Rohde, O. Schramm, Basic properties of SLE, *Ann. Math.*, to appear. Archived as math.PR/0106036 in arXiv.org.
- [22] O. Schramm, Scaling limits of loop-erased random walks and uniform spanning trees, *Israel J. Math.* **118**, 221–288 (2000). Archived as math.PR/9904022 in arXiv.org.
- [23] Q. M. Shao,  $p$ -variation of Gaussian processes with stationary increments, *Studia Scientiarum Mathematicarum Hungarica* **31**, 237–247 (1996).
- [24] W. Werner, Random planar curves and Schramm-Loewner evolutions, to appear in Springer Lecture Notes. Archived as math.PR/0303354 in arXiv.org.